Cell

Hematopoietic Origin of Pathological Grooming in *Hoxb8* Mutant Mice

Shau-Kwaun Chen,[1] Petr Tvrdik,[1] Erik Peden,[1] Scott Cho,[2] Sen Wu,[1] Gerald Spangrude,[2] and Mario R. Capecchi[1,*]
[1]Howard Hughes Medical Institute, Department of Human Genetics, University of Utah School of Medicine
[2]Department of Medicine and Pathology, University of Utah
Salt Lake City, UT 84112, USA
*Correspondence: mario.capecchi@genetics.utah.edu
DOI 10.1016/j.cell.2010.03.055

SUMMARY

Mouse *Hoxb8* mutants show unexpected behavior manifested by compulsive grooming and hair removal, similar to behavior in humans with the obsessive-compulsive disorder spectrum disorder trichotillomania. As *Hox* gene disruption often has pleiotropic effects, the root cause of this behavioral deficit was unclear. Here we report that, in the brain, *Hoxb8* cell lineage exclusively labels bone marrow-derived microglia. Furthermore, transplantation of wild-type bone marrow into *Hoxb8* mutant mice rescues their pathological phenotype. It has been suggested that the grooming dysfunction results from a nociceptive defect, also exhibited by *Hoxb8* mutant mice. However, bone marrow transplant experiments and cell type-specific disruption of *Hoxb8* reveal that these two phenotypes are separable, with the grooming phenotype derived from the hematopoietic lineage and the sensory defect derived from the spinal cord cells. Immunological dysfunctions have been associated with neuropsychiatric disorders, but the causative relationships are unclear. In this mouse, a distinct compulsive behavioral disorder is associated with mutant microglia.

INTRODUCTION

Grooming in mammals is an innate, stereotypic behavior with a well defined syntax (Berridge et al., 1987). The head is invariably groomed first, followed by body regions, and finally the anogenital region and tail. This cephalocaudal progression of grooming is defined as the "syntactic groom chain." Previous studies have shown that multiple regions of the rodent brain, notably the brainstem, striatum, and cortex are used to implement the syntactic groom chain (Aldridge et al., 1993; Berridge, 1989; Berridge and Whishaw, 1992).

Mice homozygous for a loss of function mutation in *Hoxb8* show excessive grooming. The syntax of grooming appears normal, but the number of incidences per unit time and the duration of grooming bouts are increased (Greer and Capecchi, 2002). However, the behavior is pathological, for it leads to hair removal and self-inflicted open skin lesions at the over groomed sites. This behavior is very similar to that described for humans with the obsessive-compulsive disorder (OCD) spectrum disorder trichotillomania, where compulsive removal of hair is also a hallmark. This disorder is quite common in humans with an occurrence ranging from 1.9 to 2.5 per 100 in seven separate international communities (Horwath and Weissman, 2000). Curiously, these mutant mice also excessively groom their wild-type cage mates. This aspect of the phenotype suggested that the peripheral nervous system is not likely responsible for the excessive grooming behavior (Greer and Capecchi, 2002).

Hoxb8 mutant mice also show altered response to nociceptive and thermal stimuli, which have been attributed to deficiencies in the formation and organization of interneurons in the dorsal spinal cord laminae I and II that receive the majority of nociceptive inputs (Holstege et al., 2008). Holstege et al. (2008) further suggested that the excessive and pathological grooming defects previously described in *Hoxb8* mutants result from to these sensory spinal cord defects.

It was quite unexpected that disruption of a *Hox* gene should result in a distinct behavioral deficit such as excessive and pathological grooming (Greer and Capecchi, 2002). *Hox* genes are normally involved in establishing body plans by providing positional values along the major axes of the embryo (Capecchi, 1997). However, *Hox* genes also have direct roles in the formation of multiple tissues and organs, including the formation of the hematopoietic system, and, with respect to *Hoxb8,* maintenance and differentiation of myeloid progenitor cells, one of the two known sources of microglia (Kawasaki and Taira, 2004; Krishnaraju et al., 1997; Perkins and Cory, 1993).

Since implementation of grooming in rodents is rooted within the brain, we anticipated that *Hoxb8* would be expressed in a neural circuit that modulates grooming behavior. Instead, as we report here, we have surprisingly found that, in the brain, the site that generates and implements grooming behavior, the only detectable cells derived from *Hoxb8* cell lineage are microglia. Second, we demonstrate that normal bone marrow transplantation into lethally irradiated *Hoxb8* mutant mice rescues the excessive pathological grooming behavior, without correcting the spinal cord defects. Third, conditional restriction of *Hoxb8* deletion to the hematopoietic system results in mice

with the excessive grooming and hair removal behavioral defects, without induction of the nociceptive/spinal cord defects. Finally and conversely, conditional deletion of *Hoxb8* in the spinal cord generates mice with the spinal cord sensory defects, but with normal grooming behavior.

The above experiments strongly support the hypothesis that the excessive pathological grooming behavior observed in *Hoxb8* mutant mice originates from defective microglia, thus directly connecting hematopoietic function to mouse behavior. The extensive role of microglia, as the brain's monitor and responder of immune activity, in the normal function of our brain is becoming increasingly apparent. As examples, immunological dysfunctions have been widely linked to many psychiatric disorders including OCD, major depression, bipolar disorder, autism, schizophrenia, and Alzheimer's disease (Ashwood et al., 2006; da Rocha et al., 2008; Kronfol and Remick, 2000; Lang et al., 2007; Leonard and Myint, 2009; Strous and Shoenfeld, 2006). In addition, results from genome-wide association studies suggest that genes whose dysfunction have been implicated in immune dysfunction and/or signaling contribute to increased susceptibility to the above mentioned mental disorders (Hounie et al., 2008; Purcell et al., 2009; Shi et al., 2009; Stefansson et al., 2009).

Unfortunately, animal models that directly associate distinct behavioral deficits with defective microglia have been lacking. Here we provide such a model, which should allow interrogation at the molecular genetic and cellular levels, the roles of microglia in promoting normal behavior, and how perturbation of microglia leads to pathological behavior.

RESULTS

Automated Analysis of Excessive Grooming in the *Hoxb8* Mutant Mice

Hoxb8 mutant behavior is characterized by excessive pathological grooming. Previously, we determined the number and duration of grooming bouts from continuous video recording of mouse activity (Greer and Capecchi, 2002). This procedure was robust but very labor intensive. More recently, we have been using technology developed by B.V. Metris based on the use of very sensitive vibration detectors (Laboras platforms). Each activity such as drinking, eating, rearing, climbing, locomotion, immobility, grooming, and scratching is associated with characteristic patterns of vibration, which are continuously recorded. A computer algorithm then interprets specific vibration patterns as individual behaviors. The advantage of this approach is that behavior is classified automatically and collected unobtrusively over any chosen period of time. We typically monitor activity over 24 hr periods. We have evaluated the Laboras platforms for their assessment of time spent grooming by co-monitoring mouse activity using our video camera system. The Laboras platforms are remarkably accurate, comparable to human classification and far less labor intensive. Figure S1A (available online) shows the average time spent grooming for 25 *Hoxb8* mutant mice and 22 controls over 24 hr periods as measured by the Laboras platforms. These results compare very well with those previously obtained by analyzing continuous video recordings, illustrating that on average *Hoxb8* mutant mice spend approximately twice as much time grooming as their wild-type littermates (Greer and Capecchi, 2002). The penetrance for excessive grooming in *Hoxb8* mutant mice is 100%.

Hoxb8 Cell Lineage Gives Rise to Brain Microglia

The expression pattern of *Hoxb8* in the adult brain is broad (Greer and Capecchi, 2002). However, the expression level is very low and dispersed in the brain, making it difficult to identify the cell type(s) expressing *Hoxb8*. To identify the *Hoxb8* cell lineage in the mouse brain, we generated a *Hoxb8-IRES-Cre* (*Hoxb8-ICre* onwards) driver that could be used to activate Cre-dependent *LacZ* or *YFP* reporter genes targeted to the ubiquitously expressed *ROSA26* locus (Figure S1B; Soriano, 1999). In mice carrying both the *Hoxb8-ICre* driver and *ROSA26-YFP* reporter alleles, activation of *Hoxb8* expression also triggers YFP production. Brains of such mice were collected at pre- and postnatal stages and examined by immunohistochemistry. In adult brains, YFP-positive cells can be found throughout the brain, but consistent with previous results, predominantly in the cerebral cortex, striatum, olfactory bulb, and brainstem (data not shown). These cells appear morphologically to be microglia and indeed coexpress the general microglia marker CD11b and Iba1, a marker of activated microglia (Figures 1A–1C and data not shown), indicating that *Hoxb8* is expressed in microglia or their progenitor cells. Notably, not all microglia in the brain are YFP positive, suggesting that *Hoxb8* expression was present only in a subpopulation of microglia or their progenitors (~40% of total, see Figure 7C).

In newborn mice, very few *Hoxb8*-labeled cells are observed in the brain and these cells are found predominantly in the choroid plexus (Figure 1D), meninges, and the ventricular lining, with their numbers declining with increased distance from the ventricular zone. This gradient suggests migration of YFP-positive cells from the ventricular zone into the forebrain areas. Between P2 and P14, YFP-positive cell count in the mouse brain increases dramatically and is then maintained at this high level (Figures 1E and 1F and data not shown).

Although the origin of microglia is still debated, there is general agreement that at least one subpopulation is of bone marrow origin, (i.e., derived from circulating monocytes; Kaur et al., 2001; Ransohoff and Perry, 2009). The time of first appearance and the site of entry of *Hoxb8*-labeled microglia is consistent with this subpopulation being of hematopoietic, bone marrow-derived origin.

To assess if the *Hoxb8* mutation affects the number of microglia present in the adult brain, comparable sections of the brain were evaluated for the presence of Iba1-positive cells in six *Hoxb8* mutants and six control mice. We consistently observe an approximate 15% reduction of total number of microglia present in *Hoxb8* mutant versus control mice (Figure S2). Currently, we cannot specifically label *Hoxb8* mutant (i.e., $Hoxb8^{-/-}$) microglial lineage because our *Hoxb8-ICre* driver is a "knockin" *IRES-Cre* driver, which does not itself affect *Hoxb8* function. Therefore, the above count for reduction of microglia in *Hoxb8* mutant mice may represent an underestimate of the actual reduction of the hematopoietic bone marrow-derived microglia subpopulation, should such loss be partially compensated by an increase in the resident non-*Hoxb8*-expressing microglial subpopulation.

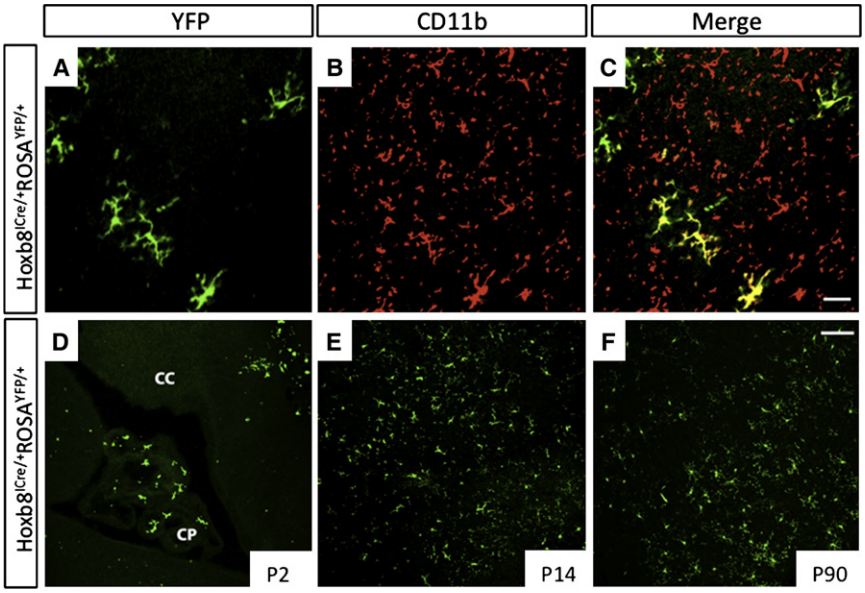

Figure 1. *Hoxb8* Cell Lineage Gives Rise to Brain Microglia

(A–F) Analysis of *Hoxb8* lineage in mice heterozygous for the *Hoxb8-ICre* and *ROSA26*-YFP alleles. To determine if cells of *Hoxb8* lineage in the brain are microglia, the identity of YFP-positive cells was examined by immunohistochemistry. Sagittal sections of the adult cerebral cortex were costained with anti-GFP antibody (A) and anti-CD11b antibody (B).

(C) Colocalization of both signals shows that these cells are microglia.

(D) Cortical microglia originating from the Hoxb8 cell lineage first appear in the brain during the first two postnatal days (P2), in the choroid plexus, and in association with the ventricular lining.

(E) The number of YFP-positive cells markedly increases by P14 throughout the cerebral cortex. This high abundance is maintained in the adult life (F).

CP, choroid plexus; CC, cerebral cortex. See also Figure S1.

The presence of *Hoxb8* lineage in the hematopoietic compartment was directly tested. Peripheral blood was collected and sorted by size and then by fluorescently labeled antibodies to cell surface antigens that distinguish the different types of white blood cells. All tested hematopoietic lineages, including platelets, granulocytes/monocytes, B cells, and T cells, exhibited *Hoxb8-YFP* signal (Figures 2A–2F). Observation of the YFP signal in both myeloid and lymphoid lineages is suggestive of *Hoxb8* expression in stem cells or multipotent progenitor cells. To further support this hypothesis, bone marrow cells from *Hoxb8-ICre/Rosa26-YFP* mice were collected and examined by fluorescence microscopy. Most of the bone marrow cells were YFP positive (Figure 2G). In addition, the *Hoxb8* -YFP$^+$ signal was present in *Sca1*$^+$*C-kit*$^+$ cells, consistent with *Hoxb8* expression in hematopoietic stem cells (Figure 2H). It has been reported that *Hoxb8* is not expressed in mature hematopoietic cells (Kongsuwan et al., 1989; Petrini et al., 1992). The above results suggest that *Hoxb8* is expressed at early stages of hematopoiesis but subsequently downregulated in fully differentiated blood cells.

Rescue of Excessive Grooming and Hair Removal Deficit in *Hoxb8* Mutant Mice by Normal Bone Marrow Transplants

We showed above that the only cells derived from *Hoxb8* cell lineage detectable in the adult mouse brain are microglia, likely of bone marrow origin. To investigate whether a dysfunction in the hematopoietic system is responsible for the *Hoxb8*-excessive grooming and hair removal phenotypes, bone marrow transplantation experiments were conducted. Four different experimental groups were included. Bone marrow cells were collected from both wild-type or *Hoxb8* mutant adult mice and transplanted into either irradiated *Hoxb8* mutant or wild-type mice at 2 months of age, respectively. The development or regrowth of hairless patches, as well as grooming times, were monitored in all mice receiving transplants over a 5 month period. In the control group, in which irradiated wild-type mice received wild-type bone marrow cells, the grooming behavior remained normal, and no hairless patches were detected for the duration of the experiment (n = 10; data not shown). In the second control group, irradiated *Hoxb8* mutant mice received *Hoxb8* mutant bone marrow. These animals showed deteriorating health, and 6 out of 11 animals in this group died before the observation period was completed, presumably due to difficulty to reestablish bone marrow with a mutant erythropoietic lineage. The surviving recipients continued to exhibit very severe grooming and self-mutilation phenotypes, without detectable hair regrowth during the observation period. Figure 3A shows one of the *Hoxb8* mutants 4 weeks after transplantation with normal bone marrow. In the group of irradiated *Hoxb8* mutant mice receiving normal, wild-type bone marrow cells, the hairless patches continued to develop for the first few weeks after transplantation. However, starting from 3 months after bone marrow transplantation, six of ten animals showed extensive regrowth of hair in the hairless areas and healing of open lesions. Four of them fully recovered and were indistinguishable from wild-type mice (Figures 3B and 3C). Grooming time was assessed on the Laboras platforms 4 months after bone marrow transplantation. The grooming times of these animals (n = 6) decreased significantly to levels comparable to those of control mice (Figure 3D). Finally, among the irradiated wild-type mice that were transplanted with bone marrow collected from *Hoxb8* mutant mice, two of ten animals developed hairless patches very similar to the phenotype observed in *Hoxb8* mutant mice (Figure 3E). These mice (n = 2) also showed increased grooming times relative to wild-type animals, but not increases as high as normally shown in *Hoxb8* mutant mice (Figure 3F).

The above experiments demonstrate that transplantation of normal bone marrow can efficiently rescue the *Hoxb8* mutant grooming phenotypes, including restoration of the hairless patches, healing of open lesions, and reduction of excessive

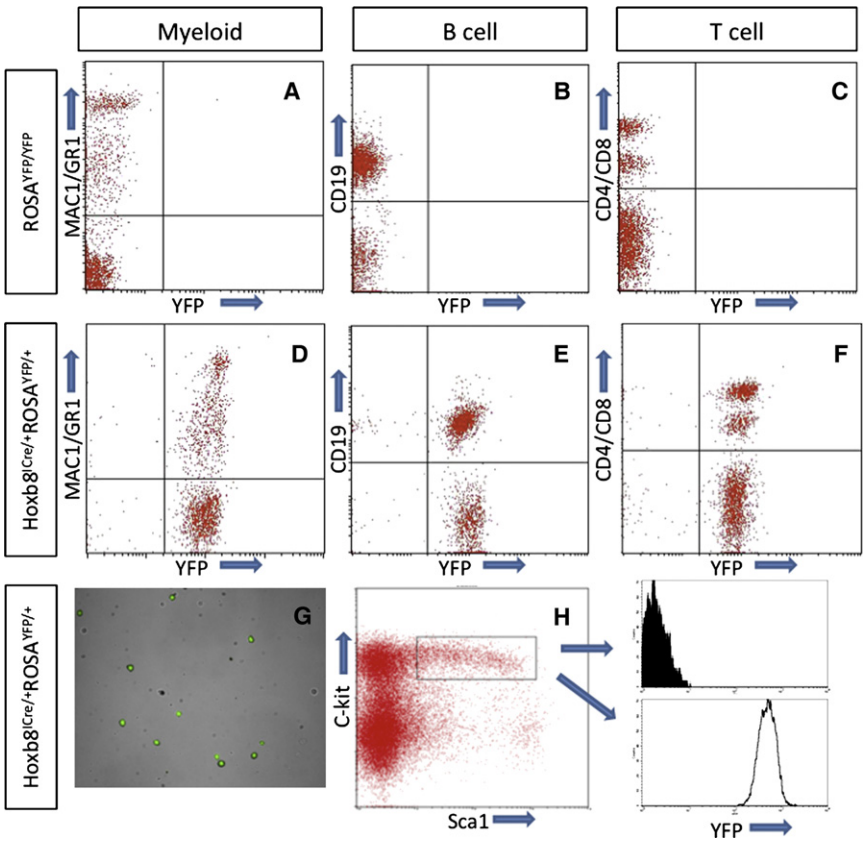

Figure 2. *Hoxb8* Cell Lineage Labels All Hematopoietic Groups Examined

(A–F) Peripheral white blood cells from *Hoxb8-ICre; ROSA26-YFP* double heterozygotes were collected and the YFP signal was examined by FACS.

(A–C) Control blood samples from *ROSA26-YFP* reporter mice in the absence of the *Hoxb8-ICre* driver.

(D–F) Analysis of blood samples collected from *ROSA26-YFP* reporter mice combined with the *Hoxb8-ICre* driver. Markers used were as follows: (A and D) Mac1/Gr-1 and YFP; (B and E) CD19 and YFP; (C and F) CD4/CD8 and YFP.

(G) YFP signal was detected by fluorescence microscopy in the majority of bone marrow cells.

(H) Most of the cells in the hematopoietic stem cell and multipotent progenitor cell domain are YFP positive. (Left) FACS analysis with Sca-1 and c-kit markers. The cells shown in the rectangle were further analyzed for YFP fluorescence. The black histogram (top right) represents YFP fluorescence detected in cells collected from *ROSA26-YFP* reporter mice in the absence of the *Hoxb8-ICre* driver, whereas the white histogram (bottom right) represents cells collected from *ROSA26-YFP* reporter mice carrying the *Hoxb8-ICre* driver.

See also Figure S2.

grooming times back to baseline. In separate experiments we have shown that *CAG-GFP*-labeled bone marrow (Ikawa et al., 1995) transferred into wild-type-irradiated mice can be detected in brain microglia 4 weeks after transplantation (Figure S3A) and increases by 12 weeks after transplantation (Figure S3B). The lower efficiency of conferring the *Hoxb8* mutant phenotype to irradiated wild-type mice following transplantation of *Hoxb8* mutant bone marrow, compared to efficient rescue of the mutant phenotype by transplantation of normal bone marrow into irradiated *Hoxb8* mutant mice, appears to be a consequence of the lower robustness of *Hoxb8* mutant bone marrow. Reconstitution of lethally irradiated wild-type mice with bone marrow containing 50% GFP labeled wild-type cells and 50% unlabeled *Hoxb8* mutant cells showed that myeloid and T cells derived from *Hoxb8* mutant bone marrows were at a measurable disadvantage relative to the normal GFP-labeled wild-type cells blood lineages (Figure S3C). In contrast, B cells derived from *Hoxb8* mutant bone marrow were at a competitive advantage relative to the wild-type cells.

Do T and B Cells Contribute to *Hoxb8*-Mediated Pathological Grooming?

The role of *Hoxb8* in hematopoiesis has not been fully elucidated. In the literature, based on experiments involving *Hoxb8* overexpression, a case has been made for *Hoxb8* involvement in the maintenance and differentiation of the myeloid progenitor pool (Kawasaki and Taira, 2004; Krishnaraju et al., 1997; Perkins and Cory, 1993). The very early expression of *Hoxb8* during hematopoiesis and our bone marrow transplantation competition studies suggest a broader role for *Hoxb8* in hematopoiesis, affecting both the myeloid and lymphoid lineages. Do T and B cells contribute to the compulsive grooming phenotype observed in *Hoxb8* mutant mice? To test this possibility, bone marrow transplantations using bone marrow derived from *RAG2* mice, which do not produce T and B cells, into irradiated *Hoxb8* mutant mice were carried out. These experiments show that *RAG2* bone marrow can rescue the excessive pathological grooming phenotype. However, the robustness of rescue is not as high as with wild-type bone marrow either in terms of the extent of hair replenishment of the hairless patches (Figures S3D and S3E) or in time spent grooming by these animals (Figure S3F). These experiments suggest that T and B cells do not have a primary role in the induction of the *Hoxb8* mutant pathological grooming phenotype, but that T and B cell deficiencies may contribute to the severity of the phenotype.

Nociceptive Defects in *Hoxb8* Mutant Mice

Holstege et al. (2008) have reported that mice mutant for *Hoxb8* show attenuated responses to noxious and thermal stimuli and display a reduction and disorganization of interneurons in laminae I and II of the dorsal horn of the spinal cord, which receive the majority of the nociceptive and thermal sensations. We have observed very similar insensitivity to noxious and thermal stimuli, as well as dorsal horn spinal cord defects in

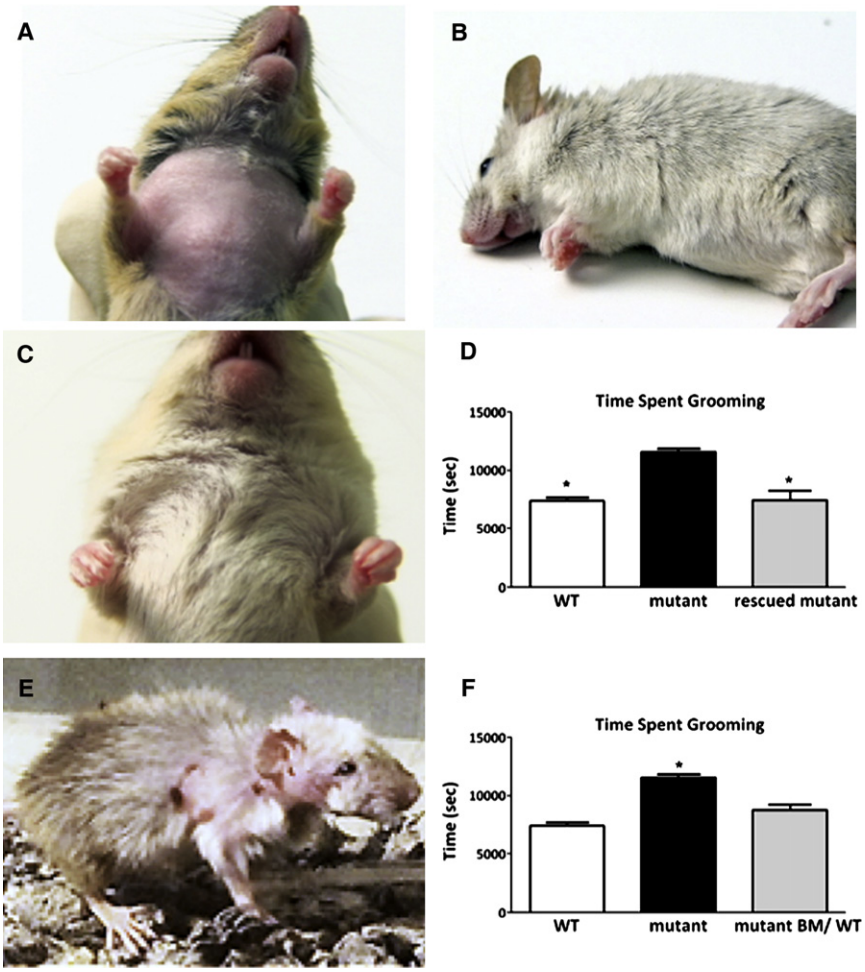

Figure 3. Rescue of Excessive Grooming and Hair Removal Defect in *Hoxb8* Mutant Mice Transplanted with Normal Bone Marrow

(A) *Hoxb8* mutant transplanted with normal bone marrow showing typical hair loss 4 weeks after transplantation.

(B) *Hoxb8* mutant mouse 3 months after transplantation with wild-type bone marrow cells showing complete recovery from hair loss.

(C) A close-up view of the ventral anterior part of the body, which is the primary region of hair removal.

(D) Laboras data collected over a 24 hr period with *Hoxb8* mutant mice transplanted with wild-type bone marrow cells show significant decrease in grooming times relative to *Hoxb8* mutant mice. White bar represents wild-type controls (n = 22) relative to *Hoxb8* mutants (n = 25). Gray bar indicates the grooming time of *Hoxb8* mutant mice rescued by normal bone marrow transplants (n = 6). All values are mean ± standard error of the mean SEM. *$p < 0.05$ versus mutant.

(E) A wild-type mouse, transplanted with *Hoxb8* mutant bone marrow, showing a hair removal and lesion pattern typical of *Hoxb8* mutant mice.

(F) Grooming times of two wild-type mice transplanted with mutant bone marrow that developed hairless patches. These experimental animals (gray column, n = 2) showed elevated grooming times, although not as long as the average observed in a large cohort of *Hoxb8* mutants. Error bars represent SEM. *$p < 0.05$ versus wild type.

See also Figure S3.

our *Hoxb8* mutant mice (Figure 4). Figures 4A and 4B show intact cervical spinal cord sections from wild-type and *Hoxb8* mutant mice stained with a general neuronal marker anti-Neu N. It is apparent from these histological sections that the number of neuronal cell bodies present in the dorsal horn of *Hoxb8* mutant mice is significantly decreased relative to those from wild-type mice. Immunohistochemical analysis of the spinal cord (shown at lumbar levels 4 and 5) further illustrate that in *Hoxb8* mutant mice, relative to control mice, disorganization and reduction in numbers are apparent in both the input sensory fibers, labeled with CGRP, as well as interneurons in laminea I and II, labeled for calbindin and calretinin (Figures 4D–4I). Nociceptive insensitivity was demonstrated by significantly greater latency time required by *Hoxb8* mutant mice to respond to heat, relative to wild-type control mice (Figure 4C). Holstege et al. (2008) further suggested that the nociceptive/spinal cord defects account for the excessive grooming and hair removal phenotypes that we previously described.

A puzzling aspect of the hair removal phenotype described by Holstege et al. (2008) is that it appears quite different from the excessive grooming and hair removal phenotype that we observe in our *Hoxb8* mutant mice. In their study, the hairless patches and skin lesions are very localized to the dorsal rump (Holstege et al., 2008) and appear more consistent with the consequences of scratching a chronic itch. We observe a gradual progression of hair removal along most of the ventral surface of the mouse and extending to the lateral surfaces, which correlates with the consequences of an excessive normal grooming pattern (see, for example, Figure 3A). The hair is removed from the overgroomed areas in our mutant mice by the use of their teeth and accumulates in between their incisors, reflecting an extension of normal grooming behavior rather than scratching with their hind paws (Greer and Capecchi, 2002). What we observe and have reported in our *Hoxb8* mutant mice is that the grooming syntax does not appear to be altered, but rather the number and duration of grooming bouts are increased. This aspect of the grooming phenotype has not been reported by Holstege et al. (2008). The marked difference in the pattern of hair removal and the excessive normal grooming observed in our mutant animals, rather than excessive scratching, suggests that the two groups might be studying different behavioral paradigms in their respective *Hoxb8* mutant mice.

Scratching in rodents is a rather simple movement made by the hind limbs (Brash et al., 2005) that can be distinguished from grooming by the Laboras platforms. To determine if our *Hoxb8* mutants exhibited excessive scratching, eight *Hoxb8*

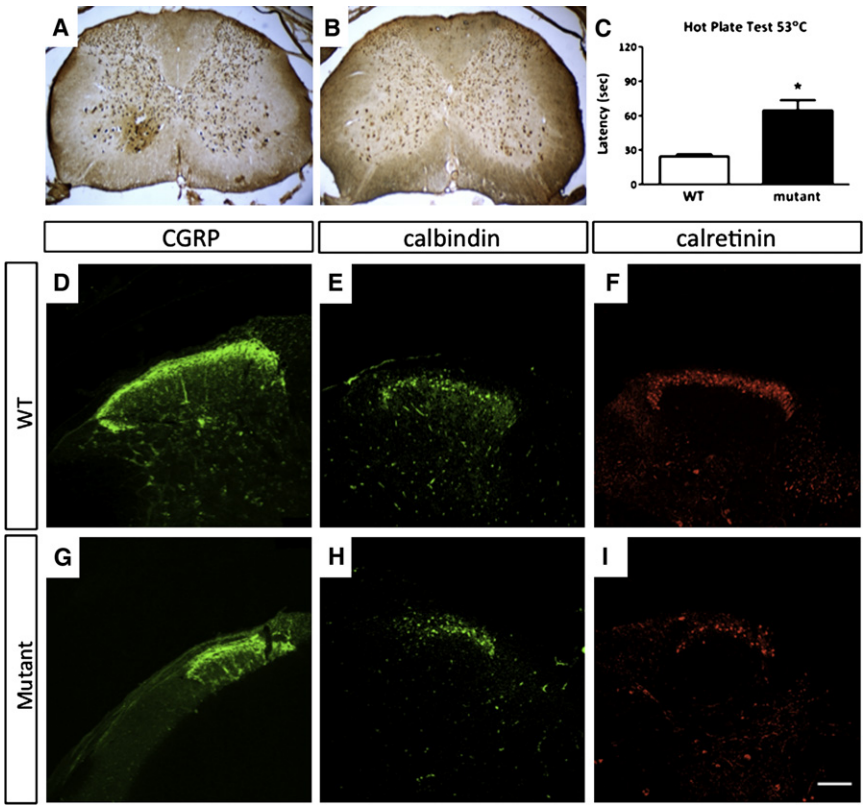

Figure 4. Anatomical and Nociceptive Defects in *Hoxb8* Mutant Mice

(A and B) Spinal cord sections at cervical levels in wild-type mice (A) and *Hoxb8* mutants (B) stained with anti-NeuN antibody. These sections are representative of wild-type and *Hoxb8* mutant sections taken along the spinal cord from C4 through the lumbar region L5. Neuron counts are decreased and the remaining interneurons are noticeably disorganized in the mutant spinal laminae.

(C) The latency of response to heat at 53°C was significantly increased in *Hoxb8* mutants. White bar, control siblings; black bar, *Hoxb8* mutant mice. Columns represent the mean ± SEM.

(D–I) Anatomical defects in dorsal spinal cord of *Hoxb8* mutant mice. Spinal cord sections shown at L4–L5 from wild-type mice (D–F) and *Hoxb8* mutant mice (G–I). The spinal cord sections were labeled with a marker for nociceptive sensory fibers (CGRP) and with interneuron markers for lamina I and II (calbindin and calretinin). The numbers of interneurons in laminae I and II are decreased and disorganized in *Hoxb8* mutant mice relative to wild-type mice. Scale bar: 100 μM. See also Figure S4.

mutants and eight wild-type mice were placed on the Laboras platforms set to score scratching. No significant differences in time spent scratching were detected between the *Hoxb8* mutant and wild-type controls (Figure S4A). Only in mutant animals that had developed severe lesions as a consequence of compulsive, excessive grooming could increased scratching begin to be observed. For comparison we provide measurements of time spend grooming over the same duration of time.

Consistent with the localized scratching caused by a response to chronic itching, Holstege et al. (2008) reported that their behavior could be alleviated by localized injection of lidocaine. We tested whether our *Hoxb8* mutant mice would respond to lidocaine treatment. Eight *Hoxb8* mutant mice and eight control sibling mice were injected with lidocaine into regions where hairless patches had developed and placed on Laboras platforms to measure their grooming periods. Lidocaine treatment did not alter the grooming behavior of either the *Hoxb8* mutant or wild-type mice (Figure S4B).

Restricted Deletion of the *Hoxb8* Gene to the Hematopoietic System Recapitulates the Excessive Grooming and Hair Removal Phenotype

The first insight that the excessive grooming and hair removal behavior could be separated from the sensory spinal cord defects in our *Hoxb8* mutant mice was gained from the transplantation experiments. Irradiated *Hoxb8* mutant mice transplanted with normal bone marrow show normal grooming behavior, but retained their thermal stimuli insensitivity spinal cord defects (Figure 5). The latency of response to thermal stimuli in the bone marrow-rescued animals was comparable to that observed in *Hoxb8* mutant mice and significantly longer than in wild-type mice. Thus, while normal bone marrow transplants into irradiated *Hoxb8* mutant mice efficiently rescued the pathological grooming defect, it did not restore the defective pain response.

To further explore the causality of the *Hoxb8* mutant phenotype, we used *Tie2 Cre/loxP*-based conditional mutagenesis. *Tie2* was originally considered an endothelial cell marker. However, Constien et al. (2001) showed that a *Tie2Cre* transgenic line displayed *loxP*-mediated recombination in all hematopoietic cells, as well as in endothelial cells. In the brain, Tie2 lineage is present in blood vessels and microglia, but not in interneurons of the dorsal spinal cord (Figure 6A and data not shown).

In order to perform tissue-specific deletion of *Hoxb8*, we constructed a conditional allele in which the entire coding sequence of this gene was flanked by *Lox511* sites (Figure S1C). Mice carrying the *Hoxb8* conditional allele were crossed to *Tie2Cre* males to produce conditional mutants. Five conditional mutants carrying *Tie2Cre* and homozygous for the *Hoxb8* conditional mutation were collected, and their grooming behavior was analyzed. Four out of the five mice developed hairless patches very similar to the patterns observed in *Hoxb8* mutant mice (Figure 6B). The grooming times, measured on the Laboras platforms, were significantly longer than control siblings and comparable to those observed in *Hoxb8* mutant mice (n = 5; Figure 6C).

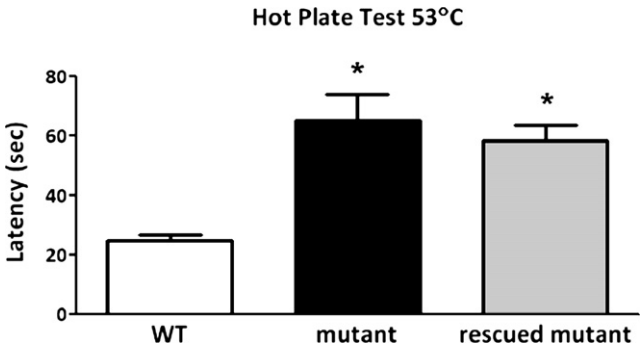

Figure 5. Nociceptive Defects in *Hoxb8* Mutant Mice Were Not Rescued by Transplantations with Wild-Type Bone Marrow

Hoxb8 mutant mice, whose pathological grooming defects were rescued by normal bone marrow transplants, still exhibit significantly longer latency of response to heat (53°C Hot Plate Test), comparable to the *Hoxb8* mutant mice. White column, wild-type controls (n = 14); black column, *Hoxb8* mutants (n = 11); gray column, *Hoxb8* mutants phenotype rescued with normal bone marrow (n = 6). Data were collected 4–5 months after bone marrow transplantation. Columns represent the mean ± SEM. *p < 0.05 versus wild-type.

However, these mice did not exhibit heat insensitivity (Figure 6D), and immunohistochemical analysis of their dorsal spinal cord laminae I and II labeled for calbindin and calretinin appeared normal when compared to *Hoxb8* mutants (Figures 6E–6J). Thus, restricted deletion of *Hoxb8* in the hematopoietic system is sufficient to induce pathological grooming in mice and, importantly, the presence of the nociceptive defects is not observed or required for induction of the aberrant grooming behavior.

Conditional Deletion of *Hoxb8* in the Spinal Cord Elicits the Nociceptive Defects but Not Pathological Grooming

Next we wanted to determine if conditional deletion of *Hoxb8* in the spinal cord recapitulates the nociceptive defects and whether or not they would be associated with the pathological grooming defects. *Hoxc8* cell lineage in the spinal cord has a broad pattern of expression very similar to that of *Hoxb8* (Figure 7A). However, relative to *Hoxb8, Hoxc8* is poorly expressed in the hematopoietic system. Most importantly, the number of *Hoxc8-ICre/Rosa26-YFP*-labeled microglia in the brain is much lower (i.e., more than 10-fold lower) when compared to *Hoxb8*-labeled cell lineage (compare, for example, Figure 7B to Figure 1F, both derived from adult cortical brain sections). Quantitation of YFP^+ $Iba1^+$ cell counts relative to $Iba1^+$ cells, which label microglia, using the respective *Hoxb8-ICre* and *Hoxc8-ICre* drivers is shown in Figure 7C. Since *Hoxc8* is strongly expressed in the spinal cord, but poorly represented within microglia, the *Hoxc8-ICre* mouse can be used to determine whether or not induction of the nociceptive defects are sufficient to initiate the pathological grooming defects. Ten such animals (i.e., *Hoxc8-ICre; Hoxb8*$^{c/c}$) were collected. None of these mutant animals developed the hair removal and skin lesion patterns typical of *Hoxb8* mutant mice (Figure 7D). Also, the time engaged in grooming by these mice was not significantly greater than in their control siblings (Figure 7E). However the latency of their response to heat was significantly longer than control siblings and was comparable to that of *Hoxb8* mutant mice (Figure 7F). Further, examination of these mutants by immunohistochemistry with calbindin and calretinin antibodies showed that ablating *Hoxb8* in the *Hoxc8* expression domain fully recapitulated the dorsal horn spinal cord defects typical of *Hoxb8* mutant mice (Figures 7G–7L). Thus, conditional deletion of *Hoxb8* in the *Hoxc8* expression domain (i.e., the spinal cord) cleanly separated the nociception/dorsal spinal cord defects from the excessive pathological grooming defects. Selective induction of the *Hoxb8*-associated nociceptive/spinal cord defects (*Hoxc8-ICre*) is not sufficient to induce the pathological grooming defects.

DISCUSSION

Herein we provide strong support for the hypothesis that the pathological grooming behavior observed in *Hoxb8* mutant mice results from a deficiency in microglia. In support of this hypothesis we have shown that the only detectable *Hoxb8*-labeled cell lineage in the brain (the source of the complex, innate behavioral grooming syntax) is microglia. Second, disruption of *Hoxb8* function results in the reduction of the total number of microglia in adult mouse brains (i.e., a microglia phenotype). Further, the excessive pathological grooming behavior in *Hoxb8* mutant mice can be rescued by transplantation with normal bone marrow. Finally, restricted deletion of *Hoxb8* in the hematopoietic system (*Tie2Cre*) recapitulates the excessive pathological grooming behavior in these mice, while restricted disruption of *Hoxb8* in the spinal cord (*Hoxc8-ICre*) does not.

There appear to be two principle sources of microglia in the mouse, a resident population that is present in the brain early during embryogenesis prior to vascularization (Alliot et al., 1999) and a second population of bone marrow origin, derived from circulating monocytes, that migrate into the brain through the vascular system shortly after birth (Kaur et al., 2001; Ransohoff and Perry, 2009). The kinetics of infiltration of *Hoxb8*-labeled microglia into the brain is consistent with this population being the bone marrow-derived subpopulation. As such, the *Hoxb8* lineage provides a useful molecular marker for distinguishing between these two microglial subpopulations. Do they have similar or different roles in the brain? Molecular markers allow genetic interrogation of the system. What would be the consequences of selectively ablating only one population? Interestingly, although *Hoxb8*-labeled microglia represent only 40% of the total microglial population present within the adult brain, selective inactivation of *Hoxb8* in this subpopulation is sufficient to induce the pathological grooming behavior. This fact would favor the hypothesis that the two microglial subpopulations present in the brain are performing distinguishable roles.

Microglia could affect neuronal activity and behavior by a number of mechanisms, including the secretion of cytokines that stimulate or inhibit neuronal activity, and work in parallel with neurotransmitters. Microglia have also been reported to function in regulating neuronal cell death during embryogenesis (Frade and Barde, 1998; Marin-Teva et al., 2004). Absence of appropriate cell death during neurogenesis could manifest itself later as aberrant behavior. Finally, the experiments of Wake et al. (2009) illustrating that microglia processes are very dynamic and

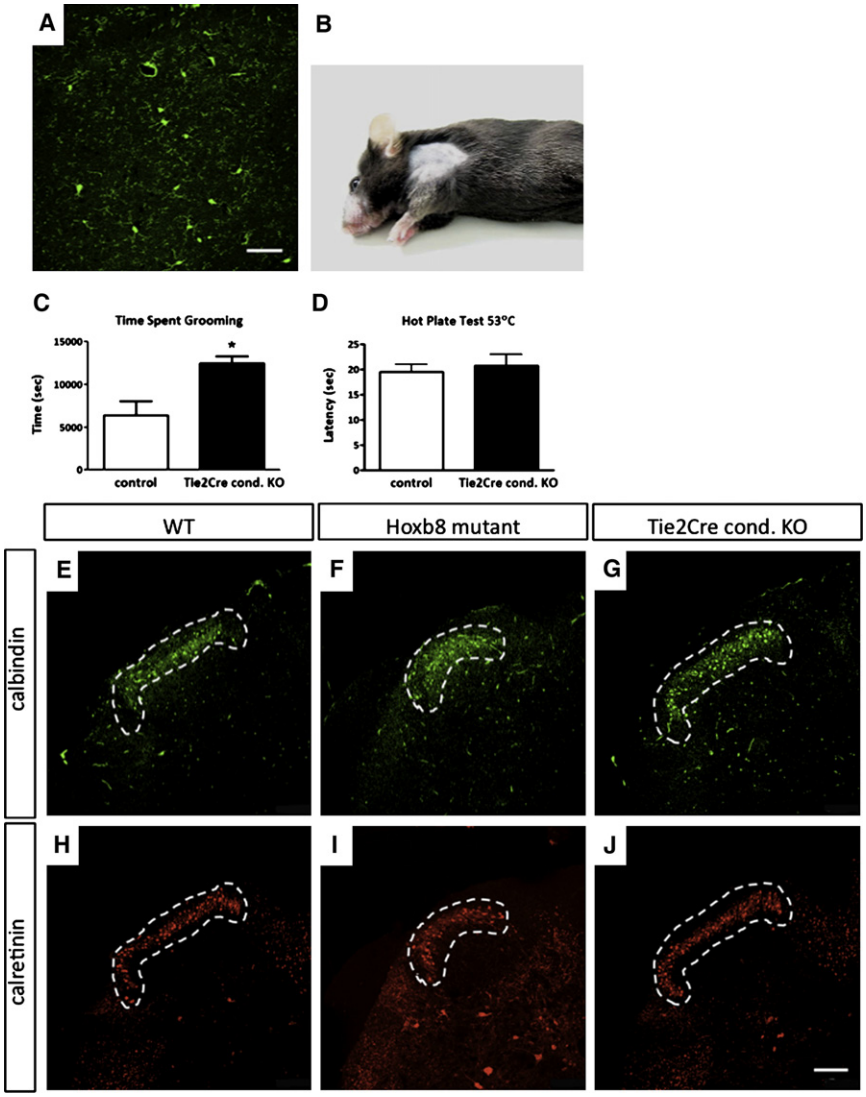

Figure 6. Mice with *Hoxb8* Deletion Restricted to the Hematopoietic System Develop Typical Excessive Grooming and Hair Removal Phenotype but not Nociceptive Spinal Cord Defects

(A) *Tie2* lineage is present in CNS microglia. Brains and spinal cords from mice carrying the *Tie2Cre* transgene and *ROSA26-YFP* allele were stained with anti-GFP antibodies. The microglial identity was confirmed by double staining with CD11b (data not shown).

(B) Conditional inactivation of the *Hoxb8* locus restricted to the hematopoietic system recapitulates hair removal and excessive grooming phenotype. Hairless patches developing in the shoulder and chest area of a 3-month-old conditional mutant mouse.

(C) *Tie2Cre* conditional mutant mice (n = 3) exhibit excessive grooming compared to control siblings (n = 5).

(D) *Tie2Cre* conditional mutant mice (black column) do not show increased latency times in response to heat relative to control mice (white bar). Error bars represent SEM. *$p < 0.05$.

(E–J) No histological defects analogous to those in *Hoxb8* mutant mice were found in dorsal spinal laminae of *Tie2Cre* conditional mutants. Spinal cord sections at L4–L5 levels were collected from wild-type mice, *Hoxb8* mutant mice, and *Tie2Cre* conditional *Hoxb8* mutants. Interneurons in laminae I and II were stained for calbindin (E–G) and calretinin (H–J). The regions with neurons positively staining for these markers are circumscribed with a white dashed boundary. Scale bar: (A) 50 μM; (E–J) 100 μM.

engage in intimate contacts with synapses are particularly intriguing. They observed that the duration of contact at synapses is dependent on neuronal activity. From the above, it is becoming apparent that due to their mobility and dynamic contacts with synapses, microglia could represent an additional system for stabilizing and managing neural networks. By virtue of their high abundance in the cortex, including the frontal orbital regions and basal ganglia, the microglia of *Hoxb8* lineage are positioned in close proximity to the pathways controlling repetitive behavior.

OCD in human patients is associated with three principal brain regions: the prefrontal cortex, particularly the orbitofrontal cortex and anterior cingulated cortex; basal ganglia, including dorsal striatum and globus pallidus; and thalamus, namely, the dorsal medial nucleus (Graybiel and Rauch, 2000; Huey et al., 2008). Excessive grooming in rodents is widely believed to mimic the key traits of OCDs. Although the syntactic grooming chain can be fully executed in rats decerebrated at various mesencephalic levels, indicating that neural circuits specifying the basic sequential structure are all present within the brainstem (Berridge, 1989), cortex and striatum play important roles in modulating the initiation and completion of grooming bouts (Berridge and Whishaw, 1992). Dopamine is a prominent neurotransmitter for implementation of the grooming pattern (Taylor et al., 2010). However, Welch et al. (2007) have reported OCD-like behaviors in *Sapap3* mutant mice that have reduced synaptic transmission in glutamanergic corticostriatal circuits, and they further showed that the compulsive grooming in these mutants is alleviated with serotonin reuptake blockers. Thus, it is apparent that multiple brain regions and signaling pathways control the frequency of repetitive behaviors.

An alternative hypothesis has been put forward that the pathological grooming observed in *Hoxb8* mutant mice is due to the sensory defects resulting from impaired formation of the spinal cord (Holstege et al., 2008). However, all of the experiments that we have presented contradict this hypothesis and have instead identified a defect in the hematopoietic system and more specifically a deficiency in microglia as likely causative for the aberrant grooming behavior. Our experiments have clearly separated the pathological grooming behavior from the sensory spinal cord defects to distinct cellular compartments.

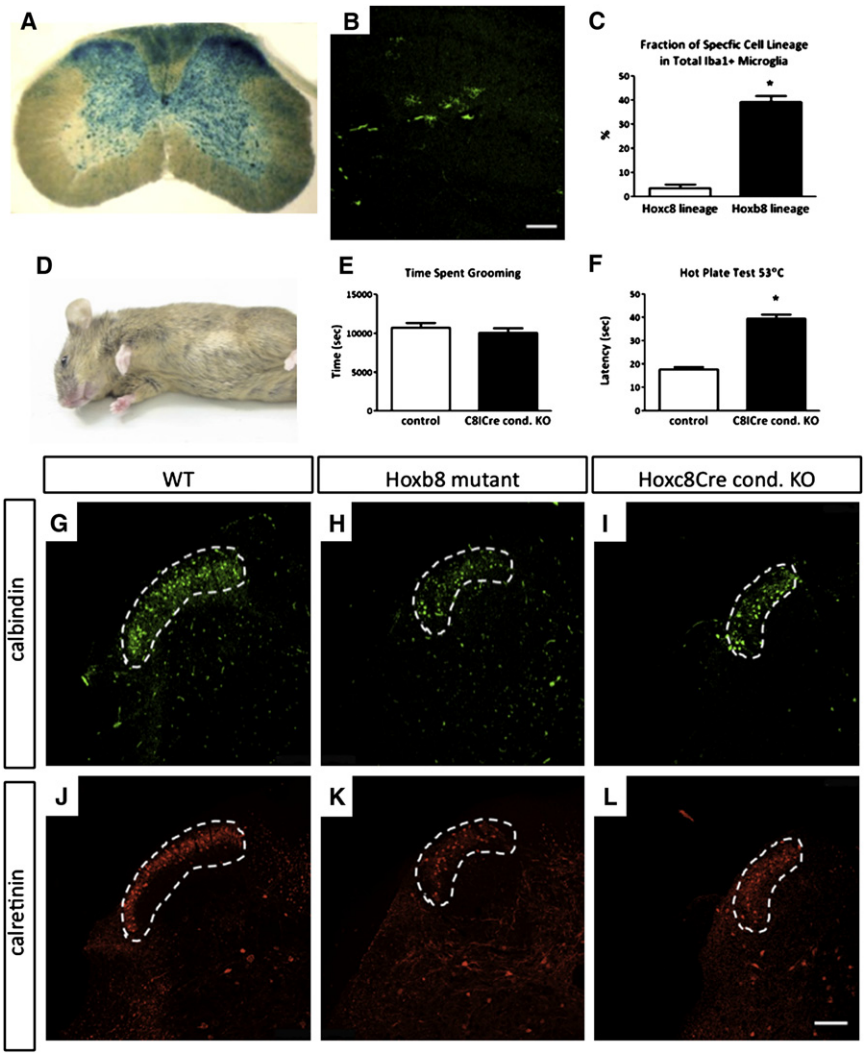

Figure 7. Conditional Deletion of *Hoxb8* in the *Hoxc8* Domain Recapitulates Nociceptive Defects but Not Excessive Grooming or Hair Removal Behavior

(A) *Hoxc8* lineage is present in all laminae of the spinal cord. X-gal staining was performed in spinal cord sections collected from mice carrying both *Hoxc8-ICre* and *ROSA26-LacZ* alleles.

(B) *Hoxc8* cell lineage in brain. Brain sections collected from *Hoxc8-ICre*; *ROSA26-YFP* mice were stained with anti-GFP antibody.

(C) Compared to the *Hoxb8* lineage, only a small percentage (<3%) of ramified microglia were labeled by the *Hoxc8* lineage. The percentage of YFP-positive cells to total ramified microglia (Iba1-positive cells) was determined from sections through the cerebral cortex derived from three *Hoxb8-ICre/Rosa26-YFP* (black column) and three *Hoxc8-ICre/Rosa26-YFP* mice (white column). The values are mean ± SEM. *$p < 0.05$.

(D) No hair removal and excessive grooming were detected in *Hoxc8-ICre* conditional mutants (10/10 animals).

(E) No significant difference in grooming time between 4-month-old *Hoxc8-ICre*-conditional *Hoxb8* mutants and control siblings were observed (n = 4). Columns represent mean ± SEM.

(F) *Hoxc8-ICre* conditional mutants exhibit heat insensitivity very similar to that observed in *Hoxb8* mutant mice. Columns represent mean ± SEM. *$p < 0.05$.

(G–L) The numbers of interneurons in laminae I and II are decreased in *Hoxc8-ICre*-conditional *Hoxb8* mutants. Spinal cord sections at L4–L5 levels were collected from wild-type mice (G and J), *Hoxb8* mutant mice (H and K), and *Hoxc8-ICre*-conditional *Hoxb8* mutants (I and L) and stained for calbindin (G–I) and calretinin (J–L). The positive regions are highlighted with a white dashed line. Scale bars: (B and G–L) 100 μM.

However, our experiments do not rule out the possibility that at later stages of the pathology the spinal sensory defects could exacerbate the consequences of excessive grooming.

Some of the apparent differences in the interpretation of *Hoxb8* mutant phenotype by the Deschamps and our laboratories may result from monitoring different behavioral features. We monitor the time spent grooming (on Laboras platforms), whereby excesses in *Hoxb8* mutant mice leads to pathological behavior and very broad hair removal and skin lesion patterns. Grooming can be distinguished from scratching by the Laboras platforms. We did not observe increased scratching in our *Hoxb8* mutant mice except modest increases at the very late stages of the pathology when lesions become apparent and the animals would normally be euthanized. The Deschamps laboratory reports very localized hair removal and skin lesions that appear more consistent with a response to a localized chronic itch. What accounts for the differences in phenotypic outcomes between the two *Hoxb8* mutant mice? Differences in genetic backgrounds is not likely to be a strong contributor since both lines have been crossed to a predominantly C57Bl/6J background.

Notably, the *Hoxb8* mutant alleles are different. This is a concern because the density of genes is very high within the *Hox* complex, and there are many noncoding RNA transcripts as well as protein-encoding transcripts transcribed within this complex (Mainguy et al., 2007). The Deschamps allele is a LacZ knockin into the first exon of *Hoxb8*. Our allele was generated by introduction of a nonsense codon in the first exon and a *loxP* site into the second. Both inserts are small relative to the LacZ insert. We have shown that a knockin allele of *neo*^{r} into the *Hoxb8* locus shows additional phenotypes due to perturbation of neighboring *Hox* gene expression, which disappear upon removal of the *neo*^{r} gene (Greer and Capecchi, 2002). Similarly, the LacZ gene could perturb neighboring RNA and/or protein expression and thereby alter phenotypes. Consistent with this interpretation, in mice homozygous for a knockin allele of *CreER*^{TM} inserted into the first exon of *Hoxb8* (Figure S1E), we have observed the localized hair removal and skin lesion phenotype described by Holstege et al. (2008) in their *Hoxb8* mutant (Figure S4D). This new phenotype shows up at a low penetrance (~10%) in addition to our characteristic *Hoxb8* mutant grooming phenotype.

We have demonstrated that a deficiency in hematopoiesis of *Hoxb8* mutant mice is causal to the pathological grooming deficit observed in these mutant animals. This deficit is correctable by normal bone marrow transplants. We have argued that the grooming malbehavior is primarily manifested by a deficit in microglia derived from bone marrow. However, a deficiency in T and/or B cells may also contribute to the severity of the behavioral pathology. Also, we have not ruled out other cellular members of the hematopoietic system as potential contributors to *Hoxb8* pathological grooming.

Why couple behavior such as grooming to the host's immune system? From an evolutionary perspective it may make perfect sense to couple a behavior such as grooming, whose purpose is to reduce pathogen count with the cellular machinery, the innate and adaptive immune systems, used to eliminate pathogens.

In summary, we have provided strong support for the hypothesis that the excessive pathological grooming behavior exhibited by *Hoxb8* mutant mice is caused by a defect in microglia. That a behavioral deficit could be corrected by bone marrow transplantation is indeed surprising. The therapeutic implications of our study on amelioration of neurological behavioral deficits in humans have not escaped us. This mouse model provides an opportunity to determine how impaired microglia results in generating such a distinct compulsive behavioral anomaly. Further, since the *Hoxb8* lineage specifically marks the microglia subpopulation derived from bone marrow, this mouse can also be used to genetically interrogate this cell subpopulation relative to the resident microglial subpopulation.

EXPERIMENTAL PROCEDURES

Mouse Lines

The lines harboring the *IRES-Cre* knockin cassettes in the *Hoxb8* and *Hoxc8* loci and the floxed, conditional *Hoxb8* allele were generated here and are detailed in the Extended Experimental Procedures.

Behavioral Analysis

Grooming times and scratching behaviors were determined on Laboras platforms (Metris B.V.). The animals were placed on the apparatus 6–8 hr before animal behavior recording started, their behavior was recorded for 24 hr periods, and the data were classified into several behavioral categories including eating, drinking, climbing, locomotion, grooming, and immobility by the Laboras software. To determine the time spent scratching, a separate testing module was used, which specifically recognizes scratching behavior. Data was collected between 8 p.m. and 12 p.m., when rodents are most active.

To measure responses to thermal stimulation, experimental animals were placed on a 53°C hot plate (Stoelting Corp.). The latency period required for the animals to respond, by licking their hind paws or by jumping, was recorded. All animal experiments carried out in this study were reviewed and approved by the Institutional Animal Care and Use Committee of the University of Utah.

Bone Marrow Transplantations

Bone marrow cells were harvested as previously described (Wang et al., 2006) and transplanted into lethally irradiated mice. Further details are provided in the Extended Experimental Procedures.

Flow Cytometry and Sorting

Peripheral blood samples were collected by retro-orbital bleeding with heparinized capillary tubes and processed as previously described (Spangrude et al., 2006). Peripheral blood cells were incubated for 20 min on ice with PE-Mac-1 and PE-Gr-1 for myeloid lineage analysis, Biotin-CD19/Avidin-APC/AF750 for B cell analysis, and APC-CD4 and APC-CD8 for T cell analysis. For bone marrow analysis, isolated immature bone marrow cells were incubated with AF647-c-Kit and PE-Sca-1 to identify early hematopoietic progenitors and stem cells. Prepared cells were analyzed with a BD FACScan flow cytometer (BD Biosciences). Additional reagents are listed in the Extended Experimental Procedures.

Statistics

All statistical analysis was performed on raw data for each group by one-way analysis of variance, followed by a Tukey's post hoc test or Student's t test. Differences among groups were considered significant if the probability of error was less than 0.05.

SUPPLEMENTAL INFORMATION

Supplemental Information includes Extended Experimental Procedures and four figures and can be found with this article online at doi:10.1016/j.cell.2010.03.055.

ACKNOWLEDGEMENTS

We thank R. Dorsky, M, Vetter, and A. Pozner for insightful discussions; C. Lenz and S. Barnett for expert help with ES cell culture; and K. Lustig for supervising the animal care. We are grateful to L. Stitzer for her assistance with manuscript preparation. M.R.C. is a Howard Hughes Medical Institute Investigator.

Received: January 23, 2010
Revised: March 3, 2010
Accepted: March 26, 2010
Published: May 27, 2010

REFERENCES

Aldridge, J.W., Berridge, K.C., Herman, M., and Zimmer, L. (1993). Neuronal coding of serial order: syntax of grooming in the neostriatum. Psychol. Sci. *4*, 391–395.

Alliot, F., Godin, I., and Pessac, B. (1999). Microglia derive from progenitors, originating from the yolk sac, and which proliferate in the brain. Brain Res. Dev. Brain Res. *117*, 145–152.

Ashwood, P., Wills, S., and Van de Water, J. (2006). The immune response in autism: a new frontier for autism research. J. Leukoc. Biol. *80*, 1–15.

Berridge, K.C. (1989). Progressive degradation of serial grooming chains by descending decerebration. Behav. Brain Res. *33*, 241–253.

Berridge, K.C., and Whishaw, I.Q. (1992). Cortex, striatum and cerebellum: control of serial order in a grooming sequence. Exp. Brain Res. *90*, 275–290.

Berridge, K.C., Fentress, J.C., and Parr, H. (1987). Natural syntax rules control action sequence of rats. Behav. Brain Res. *23*, 59–68.

Brash, H.M., McQueen, D.S., Christie, D., Bell, J.K., Bond, S.M., and Rees, J.L. (2005). A repetitive movement detector used for automatic monitoring and quantification of scratching in mice. J. Neurosci. Methods *142*, 107–114.

Capecchi, M.R. (1997). Hox genes and mammalian development. Cold Spring Harb. Symp. Quant. Biol. *62*, 273–281.

Constien, R., Forde, A., Liliensiek, B., Grone, H.J., Nawroth, P., Hammerling, G., and Arnold, B. (2001). Characterization of a novel EGFP reporter mouse to monitor Cre recombination as demonstrated by a Tie2 Cre mouse line. Genesis *30*, 36–44.

da Rocha, F.F., Correa, H., and Teixeira, A.L. (2008). Obsessive-compulsive disorder and immunology: a review. Prog. Neuropsychopharmacol. Biol. Psychiatry *32*, 1139–1146.

Frade, J.M., and Barde, Y.A. (1998). Microglia-derived nerve growth factor causes cell death in the developing retina. Neuron *20*, 35–41.

Graybiel, A.M., and Rauch, S.L. (2000). Toward a neurobiology of obsessive-compulsive disorder. Neuron *28*, 343–347.

Greer, J.M., and Capecchi, M.R. (2002). Hoxb8 is required for normal grooming behavior in mice. Neuron *33*, 23–34.

Holstege, J.C., de Graaff, W., Hossaini, M., Cano, S.C., Jaarsma, D., van den Akker, E., and Deschamps, J. (2008). Loss of Hoxb8 alters spinal dorsal laminae and sensory responses in mice. Proc. Natl. Acad. Sci. USA *105*, 6338–6343.

Horwath, E., and Weissman, M.M. (2000). The epidemiology and cross-national presentation of obsessive-compulsive disorder. Psychiatr. Clin. North Am. *23*, 493–507.

Hounie, A.G., Cappi, C., Cordeiro, Q., Sampaio, A.S., Moraes, I., Rosario, M.C., Palacios, S.A., Goldberg, A.C., Vallada, H.P., Machado-Lima, A., et al. (2008). TNF-alpha polymorphisms are associated with obsessive-compulsive disorder. Neurosci. Lett. *442*, 86–90.

Huey, E.D., Zahn, R., Krueger, F., Moll, J., Kapogiannis, D., Wassermann, E.M., and Grafman, J. (2008). A psychological and neuroanatomical model of obsessive-compulsive disorder. J. Neuropsychiatry Clin. Neurosci. *20*, 390–408.

Ikawa, M., Kominami, K., Yoshimura, Y., Tanaka, K., Nishimune, Y., and Okabe, M. (1995). A rapid and non-invasive selection of transgenic embryos before implantation using green fluorescent protein (GFP). FEBS Lett. *375*, 125–128.

Kaur, C., Hao, A.J., Wu, C.H., and Ling, E.A. (2001). Origin of microglia. Microsc. Res. Tech. *54*, 2–9.

Kawasaki, H., and Taira, K. (2004). MicroRNA-196 inhibits HOXB8 expression in myeloid differentiation of HL60 cells. Nucleic Acids Symp. Ser. (Oxf) *48*, 211–212.

Kongsuwan, K., Allen, J., and Adams, J.M. (1989). Expression of Hox-2.4 homeobox gene directed by proviral insertion in a myeloid leukemia. Nucleic Acids Res. *17*, 1881–1892.

Krishnaraju, K., Hoffman, B., and Liebermann, D.A. (1997). Lineage-specific regulation of hematopoiesis by HOX-B8 (HOX-2.4): inhibition of granulocytic differentiation and potentiation of monocytic differentiation. Blood *90*, 1840–1849.

Kronfol, Z., and Remick, D.G. (2000). Cytokines and the brain: implications for clinical psychiatry. Am. J. Psychiatry *157*, 683–694.

Lang, U.E., Puls, I., Muller, D.J., Strutz-Seebohm, N., and Gallinat, J. (2007). Molecular mechanisms of schizophrenia. Cell. Physiol. Biochem. *20*, 687–702.

Leonard, B.E., and Myint, A. (2009). The psychoneuroimmunology of depression. Hum. Psychopharmacol. *24*, 165–175.

Mainguy, G., Koster, J., Woltering, J., Jansen, H., and Durston, A. (2007). Extensive polycistronism and antisense transcription in the Mammalian Hox clusters. PLoS ONE *2*, e356.

Marin-Teva, J.L., Dusart, I., Colin, C., Gervais, A., van Rooijen, N., and Mallat, M. (2004). Microglia promote the death of developing Purkinje cells. Neuron *41*, 535–547.

Perkins, A.C., and Cory, S. (1993). Conditional immortalization of mouse myelomonocytic, megakaryocytic and mast cell progenitors by the Hox-2.4 homeobox gene. EMBO J. *12*, 3835–3846.

Petrini, M., Quaranta, M.T., Testa, U., Samoggia, P., Tritarelli, E., Care, A., Cianetti, L., Valtieri, M., Barletta, C., and Peschle, C. (1992). Expression of selected human HOX-2 genes in B/T acute lymphoid leukemia and interleukin-2/interleukin-1 beta-stimulated natural killer lymphocytes. Blood *80*, 185–193.

Purcell, S.M., Wray, N.R., Stone, J.L., Visscher, P.M., O'Donovan, M.C., Sullivan, P.F., and Sklar, P. (2009). Common polygenic variation contributes to risk of schizophrenia and bipolar disorder. Nature *460*, 748–752.

Ransohoff, R.M., and Perry, V.H. (2009). Microglial physiology: unique stimuli, specialized responses. Annu. Rev. Immunol. *27*, 119–145.

Shi, J., Levinson, D.F., Duan, J., Sanders, A.R., Zheng, Y., Pe'er, I., Dudbridge, F., Holmans, P.A., Whittemore, A.S., Mowry, B.J., et al. (2009). Common variants on chromosome 6p22.1 are associated with schizophrenia. Nature *460*, 753–757.

Soriano, P. (1999). Generalized lacZ expression with the ROSA26 Cre reporter strain. Nat. Genet. *21*, 70–71.

Spangrude, G.J., Cho, S., Guedelhoefer, O., Vanwoerkom, R.C., and Fleming, W.H. (2006). Mouse models of hematopoietic engraftment: limitations of transgenic green fluorescent protein strains and a high-performance liquid chromatography approach to analysis of erythroid chimerism. Stem Cells *24*, 2045–2051.

Stefansson, H., Ophoff, R.A., Steinberg, S., Andreassen, O.A., Cichon, S., Rujescu, D., Werge, T., Pietilainen, O.P., Mors, O., Mortensen, P.B., et al. (2009). Common variants conferring risk of schizophrenia. Nature *460*, 744–747.

Strous, R.D., and Shoenfeld, Y. (2006). Schizophrenia, autoimmunity and immune system dysregulation: a comprehensive model updated and revisited. J. Autoimmun. *27*, 71–80.

Taylor, J.L., Rajbhandari, A.K., Berridge, K.C., and Aldridge, J.W. (2010). Dopamine receptor modulation of repetitive grooming actions in the rat: potential relevance for Tourette syndrome. Brain Res. *1322*, 92–101.

Wake, H., Moorhouse, A.J., Jinno, S., Kohsaka, S., and Nabekura, J. (2009). Resting microglia directly monitor the functional state of synapses in vivo and determine the fate of ischemic terminals. J. Neurosci. *29*, 3974–3980.

Wang, H., Pierce, L.J., and Spangrude, G.J. (2006). Distinct roles of IL-7 and stem cell factor in the OP9-DL1 T-cell differentiation culture system. Exp. Hematol. *34*, 1730–1740.

Welch, J.M., Lu, J., Rodriguiz, R.M., Trotta, N.C., Peca, J., Ding, J.D., Feliciano, C., Chen, M., Adams, J.P., Luo, J., et al. (2007). Cortico-striatal synaptic defects and OCD-like behaviours in Sapap3-mutant mice. Nature *448*, 894–900.

EXTENDED EXPERIMENTAL PROCEDURES

Mouse Lines

The *Hoxb8* null mutant (Greer and Capecchi, 2002), the *ROSA26-YFP* reporter (Srinivas et al., 2001), the *ROSA26-LacZ* reporter (Soriano, 1999), the *Tie2Cre* driver (Constien et al., 2001) and the *CAG-GFP* mouse line (Ikawa et al., 1995) have been described previously. In this report, we have generated *IRES-Cre* recombinase knockins in the *Hoxb8* and *Hoxc8* loci, as well as the conditional *Hoxb8* allele. To create the *Hoxb8-ICre* allele, a 3.36 kb fragment, including the *Cre* recombinase preceded by an internal ribosomal entry site (IRES) and followed by a FRT-neo-FRT cassette, was inserted in the 3′ untranslated region (UTR) of exon 2 in the *Hoxb8* gene. A similar strategy was used to generate the *Hoxc8-ICre* allele. The *Hoxb8* conditional allele was created by inserting one *lox511* site into the 5′UTR and a second *lox511* site in the 3′UTR. For a potential temporal control of gene inactivation, the tetracycline-inducible transactivator (*IRES-rtTA2M2*) was also introduced into the *Hoxb8* 3′UTR, alongside with the FRT-neo-FRT cassette. The targeting vectors were electroporated into R1 embryonic stem cells and the successfully targeted clones were identified by Southern hybridization analysis of the *Hoxb8* and *Hoxc8* loci, using the screening strategies outlined in Figure S1. All animals used in this study had the FRT-flanked neomycin selection cassette removed by breeding with the FLPe deleter line, and the *FLPe* transgene was subsequently removed.

Lidocaine Administration

Lidocaine was applied using the method previously reported by Holstege et al. (2008). Mice were placed on the Laboras platform 2 hr before injection. Lidocaine was injected subcutaneously in the hairless regions of mutant animals, principally in the chest and shoulder areas, and to the equivalent area of wild-type control mice. The mice were placed back on the platform and rested for 15 min prior to a 30 min recording period.

Immunohistochemistry and X-Gal Staining

Mice were sacrificed by CO_2 asphyxiation and fixed via cardiac perfusion with 2% paraformaldehyde in PIPES buffer. The brains or vertebral columns were then isolated and postfixed in 2% paraformaldehyde for several hours. For spinal cord and DRG immunohistochemistry, whole vertebral columns were soaked in Immunocal solution (American Mastertech Scientific) for decalcification for 12 hr, followed by a 10 min neutralization step in solution (American Mastertech Scientific). Tissues were transferred to 20% sucrose for two days for cryoprotection, embedded in 2% gelatin and quickly frozen in liquid nitrogen. For LacZ staining, brain or vertebral tissues were sectioned at 40 or 100 μm. The sections were placed in a permeabilization solution (2 mM $MgCl_2$, 0.02% NP40, and 0.01% sodium deoxycholate in 1× PBS) for several hours, followed by an overnight incubation in X-gal developing solution (25 mM $K_3Fe(CN6)$, 25 mM $K_4Fe(CN6)\cdot 3H_20$, 2 mM $MgCl_2$, 0.02% NP40, and 0.01% sodium deoxycholate in 1 × PBS). For immunohistochemical assays, the tissues were sectioned at 20 μm. The following antibodies were used in this report: rabbit anti-GFP antibody for YFP detection (Invitrogen, 1:1000), chicken anti-GFP antibody (Aves, 1:500), mouse anti-NeuN (Chemicon, 1:100), rabbit anti-CGRP (Calbiochem, 1:100), mouse anti-calbindin (Swant, 1:5000), rabbit anti-calretinin (Swant, 1:2000), rabbit anti-Iba1 for microglia (WAKO, 1:1000), and rat anti-CD11b for monocytic lineages including macrophages and microglia (AbD SeroTec, 1: 50). Secondary antibodies were conjugated with Alexa fluorophores (Invitrogen) for immunofluorescence assays. For DAB staining, ImmPRESS peroxidase conjugated anti-rabbit Ig secondary antibody (Vector Laboratories) an ImmPACT DAB staining kit (Vector Laboratories) were used. Immunofluorescence images were captured using a Leica TCS SP5 laser-scanning confocal microscope.

Bone Marrow Transplantations

To test if *Hoxb8* mutant bone marrow was responsible for the hair loss and excessive grooming behavior, four groups of bone marrow chimeras were generated. Bone marrow cells from *CAG-GFP* mice, in which the GFP transgene is well tolerated, were used for tracking the transplanted cells in wild-type and *Hoxb8* mutant recipients. In addition, bone marrow cells from *Hoxb8* mutant mice were transplanted into *Hoxb8* mutant recipients as a control group and into wild-type recipients as an experimental group. To test if B cell or T cell functions are involved in the development of the excessive grooming phenotype, bone marrow cells from *RAG2* mutant mice were also transplanted into wild-type recipients or *Hoxb8* recipients. All donors and recipients were on a mixed C57BL/6J and Sv129 genetic backgrounds.

Bone marrow was flushed out of the tibia and femur using a syringe with Hanks' balanced salt solution containing 5% newborn calf serum (HyClone), filtered through nylon mesh, and treated with ammonium chloride solution to lyse red blood cells. Mature bone marrow cells were labeled by incubation with a cocktail of rat antibodies against mature cell markers: CD2, CD3, CD5, CD8, CD11b, Ly-6G, TER119, CD45R, CD19. Labeled cells were removed by two consecutive magnetic depletions using Dynabeads conjugated with sheep anti-rat IgG (Invitrogen Dynal).

Transplant recipient mice, at 2 months of age, were lethally irradiated (2 doses of 6 Gy, 3 hr interval) with a Shepherd Mark I ^{137}Cs source (JL Shepherd and Associates). Isolated bone marrow cells were injected by the retro-orbital route under isoflurane anesthesia at 2×10^5 donor cells in 100 μl per recipient.

Flow Cytometry and Sorting

Additional antibodies used in cell sorting protocols: monoclonal antibodies raised against CD2 (Rm2.2), CD3 (KT3-1.1), CD5 (53-7.3), CD8 (53-6.7), CD11b (M1/70), Ly-6G (RB6-8C5), TER119, CD45R (RA3-6B2), CD19 (1D3), and c-Kit (3C11) were purified from cultured hybridomas. PE-Sca-1 (D7, BD Biosciences), PE-Mac-1/CD11b (M1/70, BD Biosciences), and PE-Gr-1/Ly-6G (RB6-8C5, eBioscience) were purchased. AF647-c-Kit (3C11), Biotin-CD19 (1D3), APC-CD4 (GK1.5), APC-CD8 (53-6.7), and Avidin-APC/AF750 were conjugated in our laboratory.

SUPPLEMENTAL REFERENCES

Constien, R., Forde, A., Liliensiek, B., Grone, H.J., Nawroth, P., Hammerling, G., and Arnold, B. (2001). Characterization of a novel EGFP reporter mouse to monitor Cre recombination as demonstrated by a Tie2 Cre mouse line. Genesis *30*, 36–44.

Greer, J.M., and Capecchi, M.R. (2002). Hoxb8 is required for normal grooming behavior in mice. Neuron *33*, 23–34.

Holstege, J.C., de Graaff, W., Hossaini, M., Cano, S.C., Jaarsma, D., van den Akker, E., and Deschamps, J. (2008). Loss of Hoxb8 alters spinal dorsal laminae and sensory responses in mice. Proc. Natl. Acad. Sci. USA *105*, 6338–6343.

Ikawa, M., Kominami, K., Yoshimura, Y., Tanaka, K., Nishimune, Y., and Okabe, M. (1995). A rapid and non-invasive selection of transgenic embryos before implantation using green fluorescent protein (GFP). FEBS Lett. *375*, 125–128.

Soriano, P. (1999). Generalized lacZ expression with the ROSA26 Cre reporter strain. Nat. Genet. *21*, 70–71.

Srinivas, S., Watanabe, T., Lin, C.S., William, C.M., Tanabe, Y., Jessell, T.M., and Costantini, F. (2001). Cre reporter strains produced by targeted insertion of EYFP and ECFP into the ROSA26 locus. BMC Dev. Biol. *1*, 4.

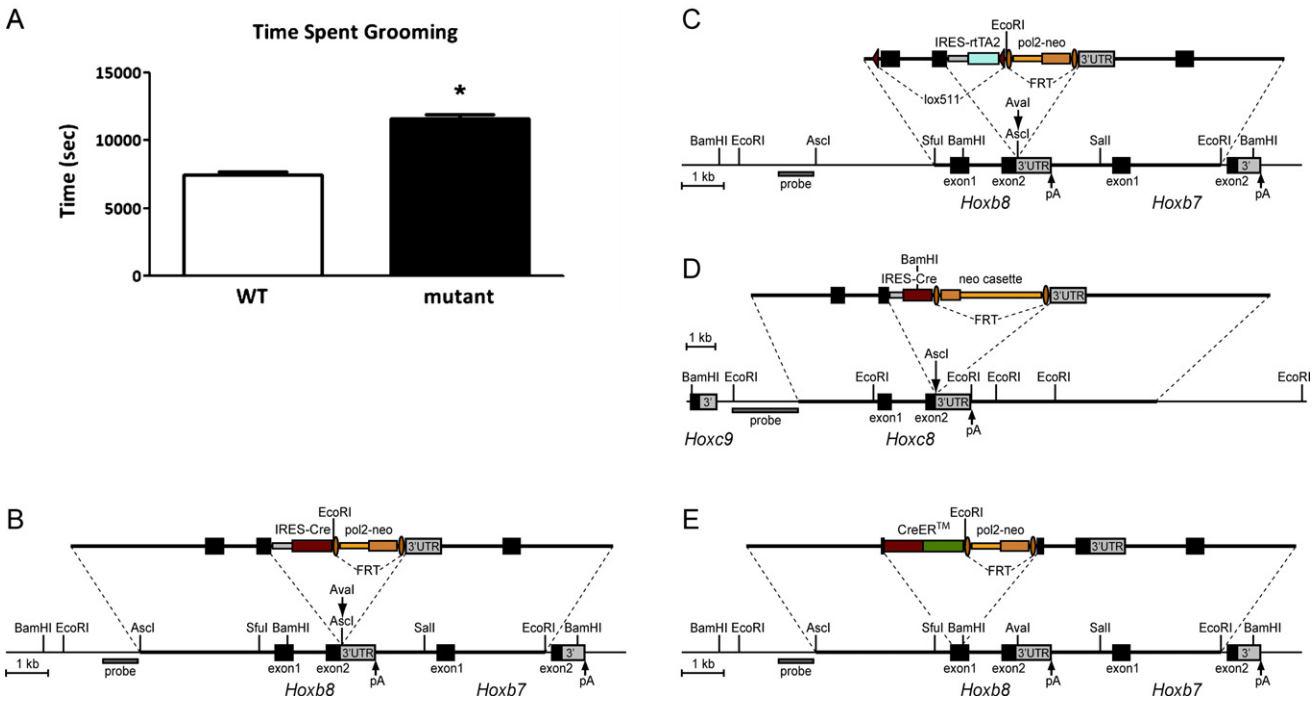

Figure S1. Automated Analysis of Grooming Behavior in Control and Hoxb8 Mutant Mice, Related to Figure 1

(A) Cumulative grooming times in 25 *Hoxb8* mutants (black column) and 22 control siblings (white column) were measured over a 24 hr period to establish the baseline values. Columns represent the mean ± SEM. *$p < 0.05$.

(B) For the *Hoxb8-ICre* allele, the *IRES-Cre* cassette was introduced in the 3′ untranslated region (3′UTR) of the *Hoxb8* gene.

(C) The *Hoxb8*^{c} conditional allele was generated by inserting lox511 sites in 5′ and 3′ UTR regions of the *Hoxb8* gene.

(D) The *Hoxc8-ICre* allele, harboring the *IRES-Cre* cassette in 3′UTR of *Hoxc8*, was made similar to the *Hoxb8-ICre* allele.

(E) *Hoxb8-CreER*^{TM} allele was prepared by replacing the *Hoxb8* exon 1 (ATG to BamHI site) with CreER^{TM} fusion that enables temporal control of lox-specific recombination in the *Hoxb8* expression domain. The external probes used in screening for accurate recombination events are indicated. All neo selection markers were flanked with FRT sites and subsequently removed by breeding with *FLPe* deleter mice. Selected landmark restriction sites are shown. pA, polyadenylation site.

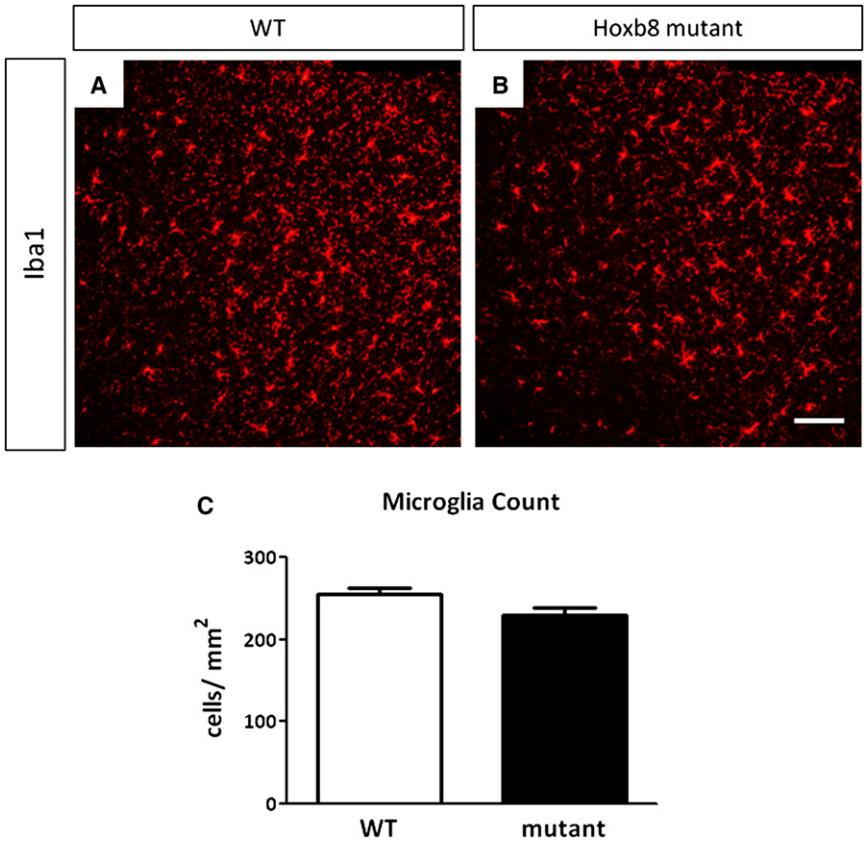

Figure S2. Microglial Density in the Forebrain of *Hoxb8* Mutants Relative to Wild-Type, Related to Figure 1

Microglial counts per area unit were determined in 4- to 6-month-old wild-type mice and *Hoxb8* mutants in comparable brain regions, including the orbital cortex, cingulate cortex, and dorsal striatum. These brain regions are known for their role in compulsive behavior.

(A and B) Iba1-positive microglia in the anterior cingulate cortex. (A) wild type (B) *Hoxb8* mutant. Scale bar: 100 μM.

(C) Comparison of microglial density in the cortex of wild type mice (white column) and *Hoxb8* mutants (black column), n = 6. The values represent mean ± SEM.

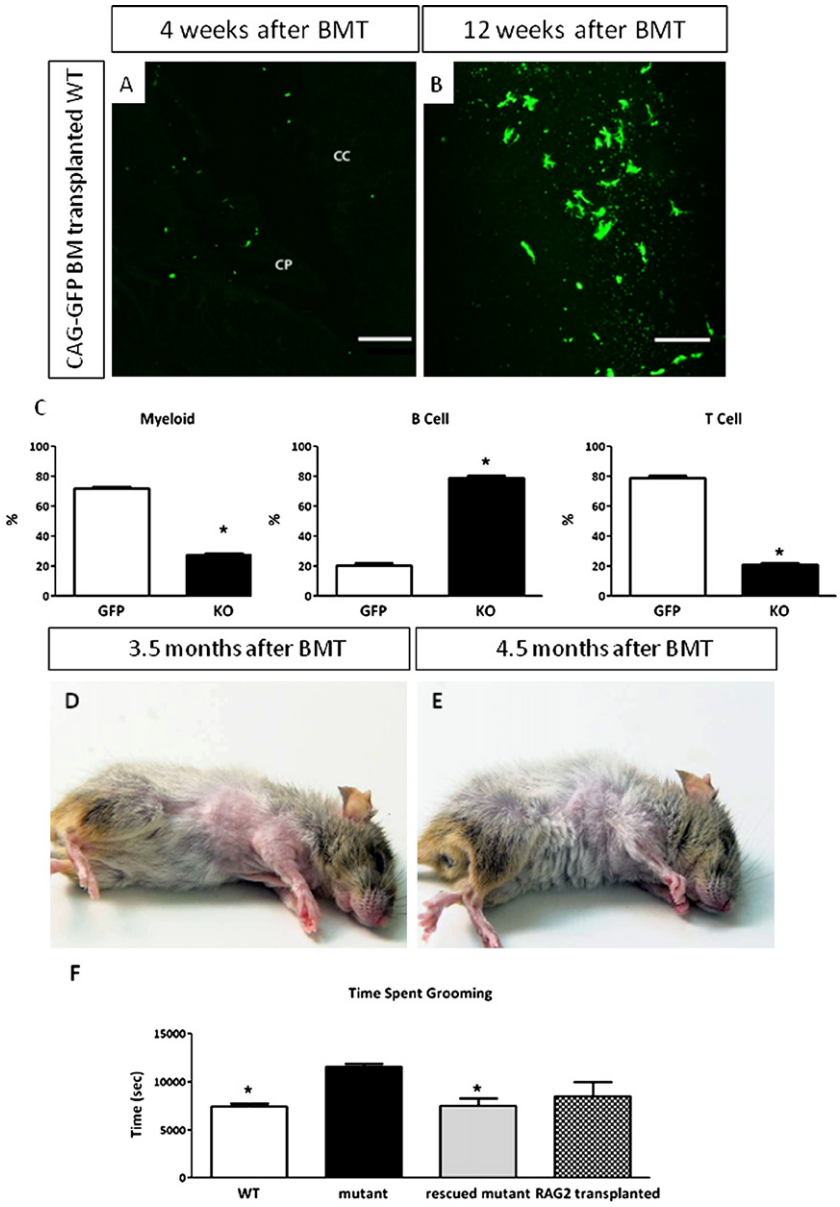

Figure S3. Cellular Dynamics of Bone Marrow Transplants, Related to Figure 3

(A and B) Infiltration of microglia in the cerebral cortex after bone marrow transplantation. Bone marrow cells were collected from *CAG-GFP* mice and transplanted to irradiated wild-type recipients. Brains of these bone marrow chimeras were dissected (A) 4 weeks or (B) 12 weeks after bone marrow transplantation, sectioned, stained with anti-GFP antibodies and analyzed with confocal microscopy. (A) Four weeks after bone marrow transplantation, only a few cells were found in the cerebral cortex, and they did not display ramified microglia morphology. CC, cerebral cortex; CP, choroid plexus. (B) Twelve weeks after bone marrow transplantation, ~30% of total microglia were GFP positive and showed ramified microglial morphology. Scale bar: 100 μM.

(C) Competitive repopulation test with bone marrow from *Hoxb8* mutant mice. Bone marrow containing 50% of *CAG-GFP*-labeled normal bone marrow cells and 50% of non-GFP *Hoxb8* mutant bone marrow cells were transplanted into irradiated wild-type recipients. Peripheral blood samples were collected 2 months after bone marrow transplantation and the percentage of GFP positive cells was determined in granulocyte/monocyte, B cell and T cell lineages. White columns represent the relative cell counts of GFP-positive cells derived from normal bone marrow. Black columns show the fractions of GFP negative cells derived from *Hoxb8* mutant bone marrow (n = 3). Columns represent the mean ± SEM. *$p < 0.05$.

(D–F) *RAG2* Mutant Bone Marrow Transplantations Rescue Hairless Patches and Reduce Excessive Grooming, Related to Figure 3. (D and E) Due to a defect in DNA rearrangement, *RAG2* mutants are B cell and T cell-deficient. When *RAG2* mutant bone marrow was transplanted into *Hoxb8* mutant mice, three out of 7 irradiated *Hoxb8* mutants exhibited hair re-growth after 3.5-months (A) or 4.5-months (B). (F) Grooming times of these bone marrow chimeras were measured on Laboras platforms 4 to 5 months after bone marrow transplantation relative to *Hoxb8* mutants (black bar) and wild type controls (white bar). Grey bar represents the grooming phenotype of *Hoxb8* mutant mice rescued with normal bone marrow. Stippled bar shows the grooming times of *Hoxb8* mutant mice rescued with *RAG2* mutant bone marrow. Columns represent the mean ± SEM. *$p < 0.05$ versus mutant.

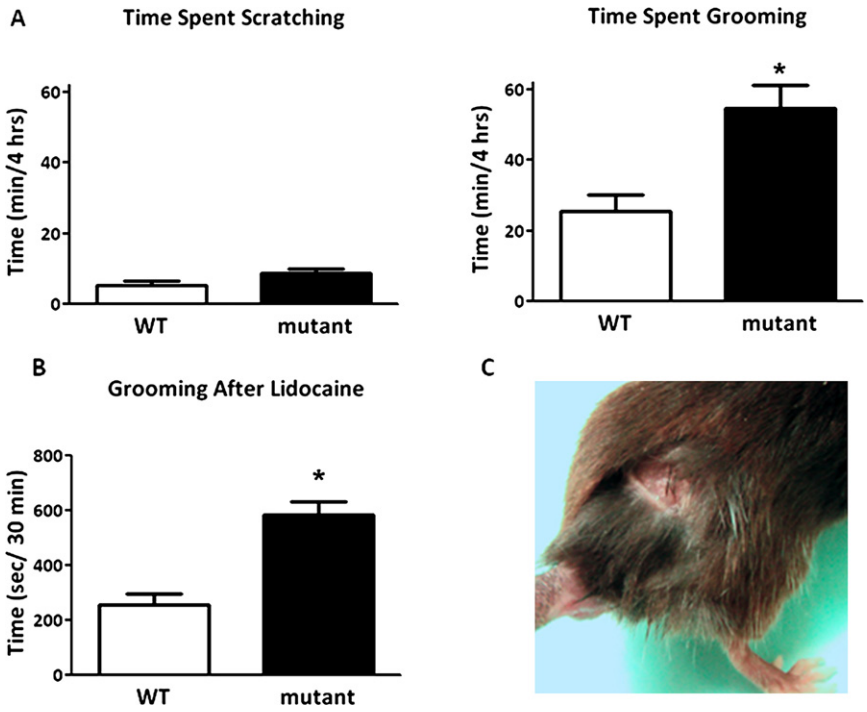

Figure S4. Characterization of Grooming and Scratching Behaviors in Regard to Sensory Defects in the Spinal Cord, Related to Figure 4

(A) Grooming and scratching can be separately analyzed by Laboras platforms. Time spent scratching in eight pairs of *Hoxb8* mutants (black columns) and wild-type mice (white) was measured in a 4 hr period. Grooming times of *Hoxb8* mutants and wild-type mice during the same period is shown for comparison. Columns represent the mean ± SEM. *$p < 0.05$.

(B) Lidocaine treatment does not alter the grooming behavior in *Hoxb8* mutant mice. Subcutaneous administration of lidocaine was performed to determine if local anesthesia would reduce the excessive grooming defect observed in *Hoxb8* mutant mice. However, the treated *Hoxb8* mutants (black column) spent approximately twice as much time grooming relative to the wild-type mice (white column), which is very similar to the differential observed in untreated *Hoxb8* mutant. Columns represent the mean ± SEM. *$p < 0.05$.

(C) Animals homozygous for the *Hoxb8-CreER^{TM}* knockin allele develop lesions in the posterior body. In this mouse line, the majority of *Hoxb8* exon 1 coding sequence was replaced with the CreER^{TM} fusion polypeptide (see Figure S2D). The CreER^{TM} knockin effectively generates a *Hoxb8* null allele, and expands the length of the *Hoxb8* gene by approximately 1.5 kb. The *Hoxb8-CreER^{TM}* mutants develop lesions in the rump and perigenital regions with a penetrance of ~10%.